BUTTERWORTH HEINEMANN

Med. Eng. Phys. Vol. 17, No. 4, pp. 297–303, 1995
Elsevier Science Ltd for BES
Printed in Great Britain

A virtual five-link model of the thumb

D.J. Giurintano*, A.M. Hollister†, W.L. Buford‡, D.E. Thompson§ and L.M. Myers¶

*Paul W. Brand Biomechanics Laboratory, Gillis W. Long Hansen's Disease Center, Carville, LA 70721, USA; †Adult Brain Injury Unit, Rancho Los Amigos Medical Center, Downey, CA, USA; ‡Orthopedic Biomechanics Laboratory, University of Texas Medical Branch, Galveston, TX, USA; §Department of Mechanical Engineering, University of New Mexico, Albuquerque, NM, USA; ¶Department of Anatomy, University of Washington, Seattle, WA, USA

Received February 1994, accepted June 1994

ABSTRACT

Most researchers have modelled the thumb as three rigid links with connections of two universal joints (carpo-metacarpal joint and metacarpo-phalangeal joint), and a hinge joint (interphalangeal joint). Although this produces the required number of degrees of freedom, the resulting motion is not anatomically accurate. In this work, the thumb is modelled as a five-link manipulator with the virtual links connected by hinge joints – one for each degree of freedom of the thumb. The axes of the hinges are not orthogonal to one another, to the long axis of the bones or to the anatomic planes. Four static positions of hand function were analysed – key pinch, screwdriver hold, tip pinch, and wide grasp. The virtual five-link model of the thumb predicted similar muscle recruitment patterns to published EMG data. The force at the distal surface of the trapezium is between 6 and 24 times the applied load depending on the posture.

Keywords: Thumb mechanics, kinematics, mathematical modelling

Med. Eng. Phys., 1995, Vol. **17**, 297–303, June

NOMENCLATURE

$[Tr]$	translation matrix
$[Rox]$	rotation about x-axis
$[Roy]$	rotation about y-axis
$[Roz]$	rotation about z-axis
F	Force
M	Moment
f_i	muscle force
σ_i	muscle stress
$[A-A\ Rot]$	Rotation matrix resulting from abduction–adduction motion
$[F-E\ Rot]$	Rotation matrix resulting from flexion–extension motion
$[A-A\ axis]$	Matrix transformation to orient the abduction–adduction axis $[Tr\ A-A] * [Roy\ A-A] * [Roz\ A-A]$
$[F-E\ axis]$	Matrix transformation to orient the flexion–extension axis $[Tr\ F-E] * [Rox\ F-E] * [Roz\ F-E]$
$[T_1]$	Total matrix transformation for control points associated with the metacarpal
$[T_2]$	Total matrix transformation for control points associated with the proximal phalanx
$[T_3]$	Total matrix transformation for control points associated with the distal phalanx
CMC	carpo-metacarpal
MP	metacarpal-phalangeal
IP	interphalangeal
FPL	flexor pollicis longus
FPB	flexor pollicis brevis
EPL	extensor pollicis longus
EPB	extensor pollicis brevis
OPP	opponens pollicis
APL	abductor pollicis longus
APB	abductor pollicis brevis
ADP	adductor pollicis
FDI	first dorsal interosseous

Work performed at: Paul W. Brand Biomechanics Laboratory, Gillis W. Long Hansen's Disease Center, Carville, LA 70721. For information contact: David J. Giurintano

INTRODUCTION

The musculoskeletal system has been studied for many years with the purpose of understanding the function of the system and determining methods of correcting dysfunction due to accident or disease. Because of its importance to essential daily activities, the mechanics of the thumb has been investigated by many researchers.

The accuracy of the kinematic model of the joints used in the analysis of thumb kinetics is extremely important since the calculations for muscle and external forces are all made relative to the kinematic structure. Chao *et al.*[1] and Cooney *et al.*[2] analysed the tendon forces and joint reactions in the thumb for five positions – tip pinch, lateral pinch, grasp, ulnar pinch (finger), and palmar pinch (thumb). In their model, the carpo-metacarpal and metacarpal-phalangeal joints were modelled as universal joints oriented along the anatomic planes. The interphalangeal joint was modelled as a hinge joint perpendicular to the sagittal plane of the thumb. These models do not account for the rotation which occurs with movements at all three joints, and abduction and adduction which occurs at the IP joint.

The anatomic work of Hollister *et al.*[3] and the computer simulations of Buford *et al.*[4] suggest a model in which the axes of rotation are not perpendicular to the bone or to each other (*Figure 1*). The CMC joint has two axes, one in the trapezium and one in the metacarpal. The MP joint has two offset axes, one in the metacarpal and one which moves with the proximal phalanx. The IP joint has a single axis which is offset in two planes. The axes of rotation offset from the anatomic planes produces the observed conjunct rotations such as pronation and supination which occur with normal thumb motion. Motion about these axes results in congruent joint motion in the computer simulation. With this kinematic model, the thumb can be modelled as a virtual five-link manipulator. The links are connected by hinge joints, one link for each axis of rotation. While this system has the same number of degrees of freedom as previous models, the kinematic relationships are quite different.

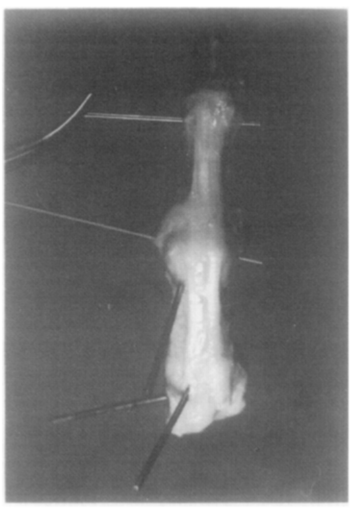

Figure 1 Cadaver thumb with non-orthogonal axes determined experimentally by the axis finder method. The CMC joint flexion–extension axis intersects the trapezium and travels parallel to the trapezium's body. The CMC joint abduction–adduction axis intersects the metacarpal just distal to the dorsal and volar beaks. The MP joint flexion–extension axis passes just palmar to the epicondyles, through the origin of the collateral ligaments. The MP joint abduction–adduction axis intersects the volar plate between the sesamoids. The IP joint flexion–extension axis passes through the origin of the collateral ligaments and Cleland's ligaments

If the CMC and MP joints are modelled as joints whose axes intersect and are perpendicular to each other (universal joints) and oriented along the anatomic planes but experimental results show that the axes do not intersect and are not perpendicular, then the past models do not represent the normal anatomy. The position of the bones of the thumb with respect to the hand and to themselves cannot be accurately simulated for various functional positions. Similarly the IP joint cannot be modelled as a hinge joint perpendicular to the sagittal plane of the thumb when its axis of motion is not perpendicular to the sagittal plane. Accurate placement of the distal phalanx with respect to the proximal phalanx cannot be achieved. Therefore, the direction of the muscles' lines of action and the orientation of the applied load with respect to the thumb are not correct if accurate kinematic models are not used.

METHODS

The virtual five-link model assumes the thumb to be composed of five links. Although this appears to be unlike the physical system which is composed of three links (bones), the physical system has embedded axes of motion which co-articulate on one surface but which are both physically real and separated from one another. The virtual links are connected together with hinge joints. The axes of motion of the hinges are not perpendicular to the links. The virtual five-link model of the thumb is depicted in *Figure 2* with the relationship between the joint axes, the virtual links, and the lines of action of the muscles and the applied load represented. The motion of the bone segments is linked to anatomic axes as determined by Hollister *et al.*[3] An example of a cadaver thumb with the axes of motion determined is depicted in *Figure 1*. The most proximal pin represents the location and orientation of the flexion–extension axis of the CMC joint in the trapezium. The next distal

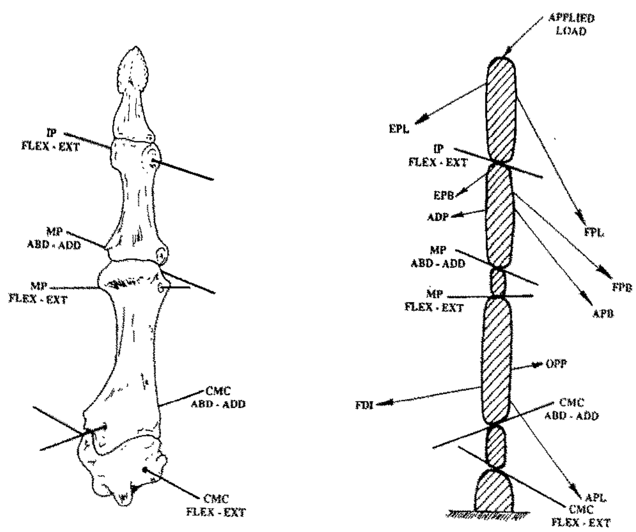

Figure 2 Virtual five-link model of the thumb with the joint axes labelled, lines of action of the muscles and the applied load represented. EP; Extensor pollicis longus: FPL; Flexor pollicis longus: EP; Extensor pollicis brevis: ADP; Adductor pollicis: FBP; Flexor pollicis brevis: APB; Abductor pollicis brevis: OPP; Opponens pollicis: FDI; First dorsal interoseous: APL; Abductor pollicis longus

pin represents the location of the abduction–adduction axis of the CMC joint in the proximal end of the metacarpal. The two pins located in the distal end of the metacarpal represent the locations of the flexion–extension (the more proximal pin) and the abduction–adduction (the more distal pin) axis of the MP joint. The pin located in the distal end of the proximal phalanx represents the location of the flexion–extension axis of the IP joint.

Homogeneous matrix transformations are used to move the bones and the tendon control points from their resting posture, $P - [x\ y\ z\ 1]$, to the four functional positions, $P' - [x'\ y'\ z'\ 1]$, investigated—key pinch, screwdriver hold, tip pinch, and wide grasp. This is described as

$$P' = [T_i] * P. \tag{1}$$

The concatenated transformation for control points associated with the metacarpal was

$$[T_1] = [A - A\ axis] * [A - A\ Rot] * [A - A\ axis]^{-1} * [F - E\ axis] * [F - E\ Rot] * [F - E\ axis]^{-1} \tag{2}$$

The concatenated transformation for control points associated with the proximal phalanx was

$$[T_2] = [A - A\ axis] * [A - A\ Rot] * [A - A\ axis]^{-1} * [F - E\ axis] * [F - E\ Rot] * [F - E\ axis]^{-1} * [T_1]\,, \tag{3}$$

and for the control points associated with the distal phalanx the concatenated transformation was

$$[T_3] = [F - E\ axis] * [F - E\ Rot] * [F - E\ axis]^{-1} * [T_2]\,. \tag{4}$$

These matrix transformations are for rotation about an arbitrary axis in space (which is

$$[F - E\ axis] * [F - E\ Rot] * [F - E\ axis]^{-1} \tag{4a}$$

for a flexion–extension axis).

Control points are all points logically associated with a bone segment. They define the lines of action of the muscles and the paths of the tendons. Thompson and Giurintano[5] used a building block approach to construct tendon models for the long flexors of the hand. From that work two building blocks will be used in this research. Two additional building blocks will be added. Building block *A* simulates a tendon travelling in a straight line. The tendon control points are transformed by all of the translations and rotations of the bone segment to which the sheath is connected. Building block *B* simulates a tendon travelling in a circular path as it crosses a joint. Landsmeer's[6] third model is the basis of this simulation.

Two additional building blocks were developed for this work. Building block *E* is used to simulate an extensor tendon's dorsal travel over a joint in a circular arc with the radius of the arc equal to 1.3 times the distance between the two points on the circle. The value of 1.3 was determined heuristically to give the proper radius of curvature for tendons as they pass over the dorsal surface of the MP joint capsule. Building block *F* simulates the EPB and EPL tendons' dorsal travel over the IP joint in an arc modelled as a fourth order polynomial ($Y = A * X^4 + B * X^2 + C * X + D$). The polynomial was chosen as the lowest order polynomial which would yield both spatial continuity and first derivative continuity for the tendon path. This model was used at both the proximal and distal segments. Building block *F* also simulates the insertion of the FPL into the distal phalanx.

Each muscle's line of action was constructed using building blocks *A*, *B*, *E*, and *F*. This line of action is inherent in the control points used to logically tie the structure into the kinematic hierarchy. These points were chosen from observation made during dissections to yield the proper tendon geometry at the joint. The FPL pattern is *ABAF*; the EPL is *EAFAF*; the EPB is *EAFA*, and the FPB , the OPP, the APL, the APB, and the FDI *A*. The information generated from the locations of the control points of the muscle-tendon units of the thumb is used to graphically display their paths. The information also generated the proper lines of action of the forces exerted by the muscle-tendon units across the joints.

In order to resolve the distribution of forces generated by the muscles of the thumb and determine the joint reactions at the CMC, MP and IP joints, optimization techniques must be used. The relationships of the model are so complex that they preclude an analytical solution. Even the computation of derivatives is intractable and thus a non-derivative technique was employed. The redundancy problem occurs from the attempt to solve the system of 30 equations with 34 unknowns. There are 6 equations for each hinge joint with 25 unknown joint reactions (5 for each hinge joint—3 components of the force and 2 components of the moment) and 9 unknown muscle forces. From observation of the 30 equations, only the equations for summation of moments about the hinge axis (in local coordinates) need to be solved using optimization techniques. In the local coordinates, the hinge axis was aligned along the *x*-axis for flexion–extension and along the *y*-axis for abduction–adduction. If the muscle forces are known, then the joint reactions can be uniquely determined. If all 30 equations are used, then redundant solutions are determined. Therefore, this system is solved by the non-linear optimization techniques developed by McPhate[7] after Powell[8]. This routine employs a conjugate gradient method for optimizing functions without the necessity of calculating derivatives. It can be descriptively represented by the method of parallel tangents in two dimensions. Only the five moment equations for the summation of moments about the local hinge axis are needed to constrain the optimization. The formal definition of the force analysis of the virtual five-link model of the thumb is

$$\text{minimize } \sum \sigma_i^2$$

$$\text{subject to } \sum_{f_i \geq 0} M_{hinge\ axis\ (local\ coordinates)} = 0 \tag{5}$$

where σ_i the muscle stress, of the *i*th muscle is defined as the force of the *i*th muscle divided by its physiologic cross-sectional area. The physiologic cross-sectional area for the muscles was determined by Brand *et al.*[9] The objective function was chosen from the work of Crowninshield and Brand[10]. They proposed a non-linear optimization method to resolve the redundancy problem. The endurance of musculoskeletal function was maximized. The use of non-linear optimization techniques does not guarantee that the final solution is a global minimum to the problem. The cost function is convex, however, and therefore global convergence is guaranteed.

From the conceptual model of *Figure 2*, free body diagrams were constructed initially from the most distal link, then the two most distal links, until five free bodies were created. From these free body diagrams, the equations of static equilibrium were generated. Soft tissue effects were neglected. The analysis performed in this paper is on a thumb with normal (healthy) joints. Disease states could also be modelled with the virtual five-link model by modifying the location and orientation of the axes. The simulation allows the user to specify the magnitude of the applied load. For this study four functional positions are modelled. In key pinch, the applied load is acting upon the pulp. For the screwdriver hold, the applied load acts at a 60 degree angle to the distal phalanx's tip. The applied load is acting through the distal phalanx for the tip pinch orientation. In wide grasp, the applied load acts on the ulnar side of the distal phalanx.

With the muscle forces generated from the optimized solution for the virtual five-link model, the forces and moments on the distal surface of proximal phalanx, metacarpal, and the trapezium are calculated. By using static force analysis in conjunction with the knowledge of the three-dimensional locations of the lines of action of the muscle-tendon units and the location of the joint surfaces, the joint reactions on the distal surface of the bones can be determined.

The muscle forces for solution of the equilibrium equations are calculated by the solution of the virtual five-link analysis. The lines of action for the muscle are calculated from the three-dimensional data from the CT images.

RESULTS

The results predicted by the virtual five-link model for muscle-tendon forces and joint reactions are for an applied load of 10 N (*Tables 1–2*). The joint reactions (at the distal surface of each bone) are calculated from the free body analysis of the physical bones not the virtual links (*Table 2*).

In key pinch, the FPL, the FPB and the EPB stabilize the thumb against the applied load. For the screwdriver hold, the EPL, the FPL, the FPB, the EPB and the APB are used to stabilize the thumb. For tip pinch, the FDI and the ADP (adductors), the FPL, and the APL stabilize the thumb. In wide grasp, the EPB, ADP and OPP stabilize the thumb. In each of the postures, agonists are activated to oppose the applied load, and antagonists are activated in concert with the agonists to stabilize the thumb.

The force applied to the distal surface of the trapezium as a result of the thumb muscles firing to stabilize an applied load is between 6 and 24 times the applied load depending on the posture. The distal surface of the metacarpal experiences similar loads. The loads applied to the distal surface of the proximal phalanx are reduced by one-half to one-fifth of the loads applied to the metacarpal. The reactions at the surface of the trapezium consist of contributions due to shear in addition to compression. At the surfaces of the metacarpal and the proximal phalanx, load is directed primarily in compression. The direction of the reaction moments varies with each posture relative to each bone's surface (*Figures 3–6*). The bones for the anatomic structure come from CT image processing described in Myers *et al.*[11] The force vectors are represented with single headed arrows, and the moment vectors are represented with double headed arrows.

DISCUSSION

Many methods have been used to compute the muscle forces and joint reactions for normal thumb function. The problem is difficult because of the complexity of the system—multiple muscle-tendon units that cross several joints, variable applied loading to the digit and the intricate joint articulations. In order to solve the problem, previous studies introduced the simplifications of two-dimensional analysis, using only some of the involved muscles, and applying simplistic mechanical joint models. The virtual five-link model presented here is a new analysis of the thumb modelled as a five-link manipulator. This model is based on a kinematic structure of the thumb consisting of five virtual links connected by hinge joints. The axes of the hinges are not orthogonal to one another, to the long axis of the bones or to the anatomic planes. This construction represents the axes determined experimentally by Hollister *et al.*[3] Four tendon building block models are used to define the path of the thumb muscle-tendon units with respect to the bones. With this model, four hand postures were analysed to determine which muscles stabilized the thumb and the reactions at the proximal surfaces of the joints. This model differs from previous models which consisted of two universal joints and a hinge joint connecting the phalanges. With the virtual five-link model, there is an anatomic relationship between the muscles and the axes of motion of the thumb.

Tendons are modelled as inextensible chords, therefore the dissipation of any force used to lengthen the tendons due to their elastic nature has been ignored. If the joints are destroyed due to osteoarthritis or rheumatoid arthritis, then motions other than rotations about these fixed axes may occur; therefore, the degrees of freedom of the thumb may be altered. For an interposition arthroplasty, the modified CMC joint may best be modelled as a spherical joint whose centre is at

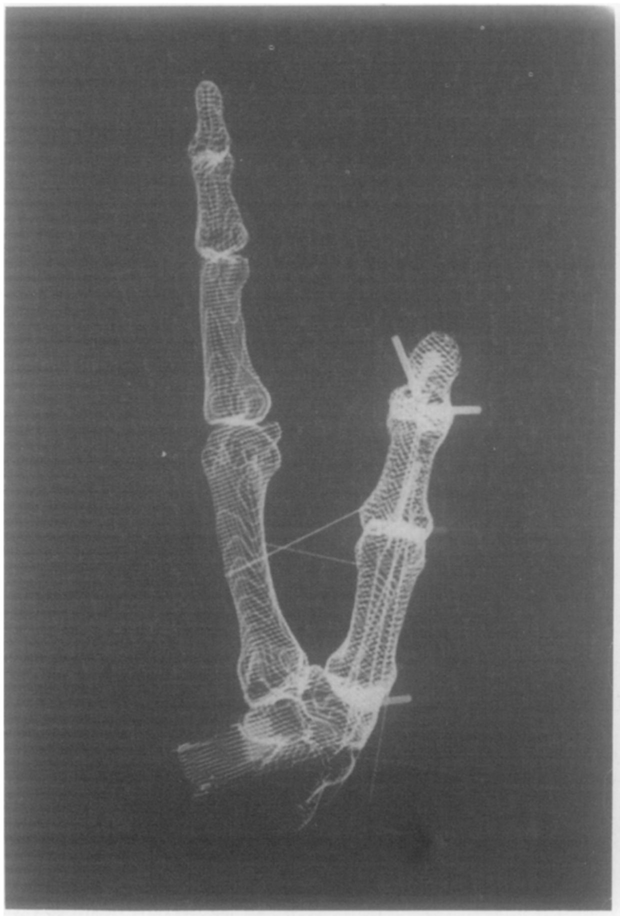

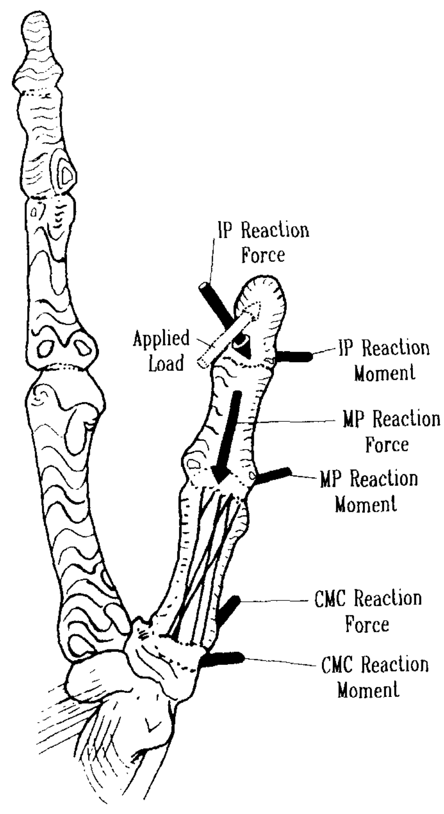

Figure 3 Computer visualization of the directions of the joint reactions for the 'key pinch' posture solved for an applied load of 10 N. Force vectors are represented with single headed arrows, and moment vectors are represented with double headed arrows

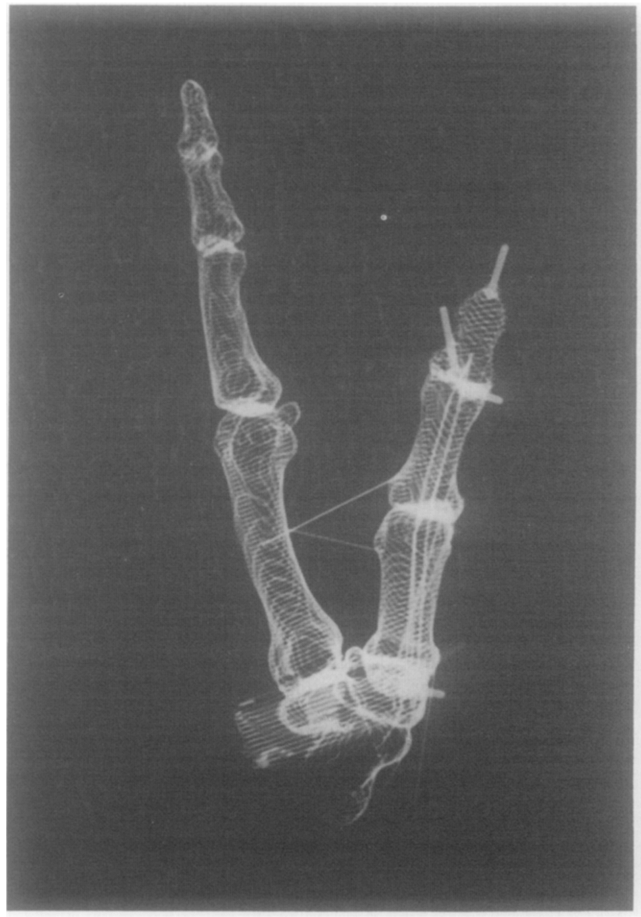

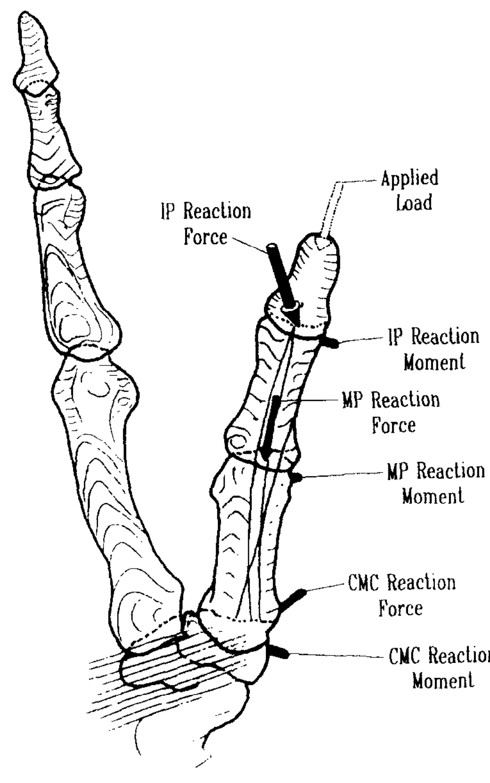

Figure 4 Computer visualization of the direction of the joint reactions for the 'screwdriver hold' posture, solved for an applied load of 10N. Symbols as *Figure 3*

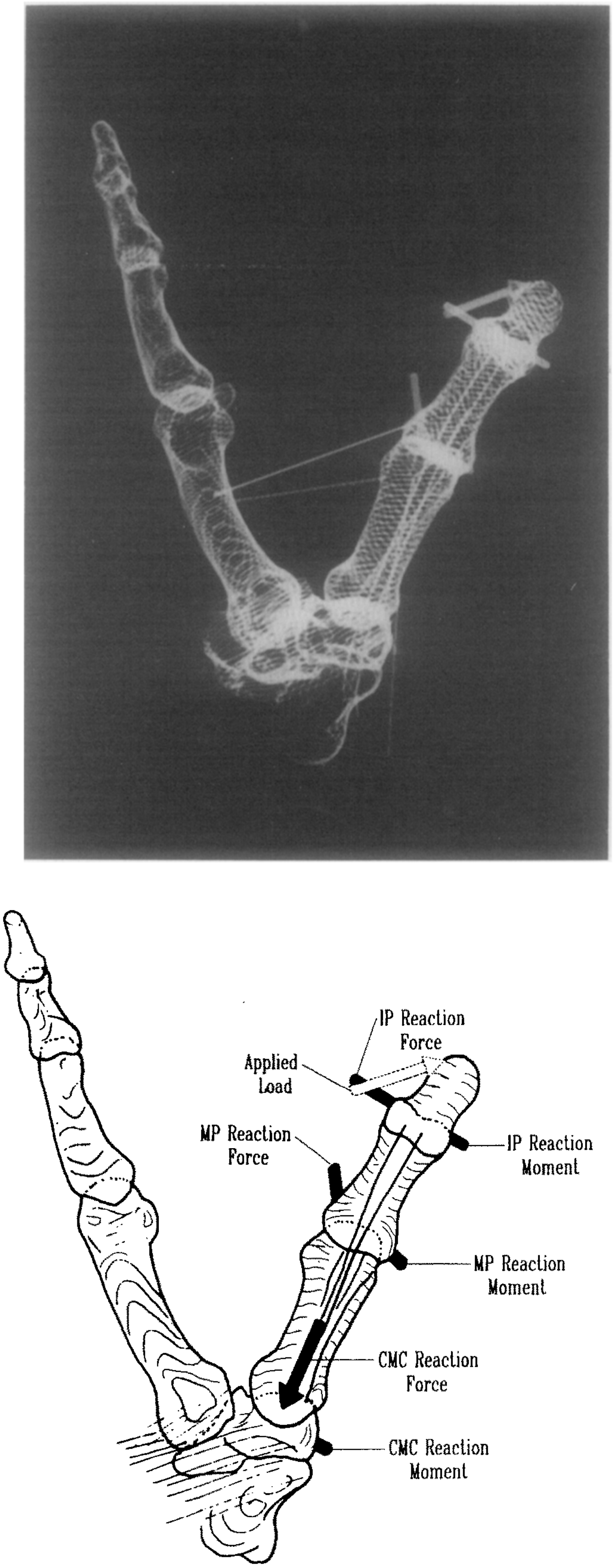

Figure 5 Computer visualization of the directions of the joint reactions for the 'tip pinch' posture, solved for an applied load of 10N. Symbols as *Figure 3*

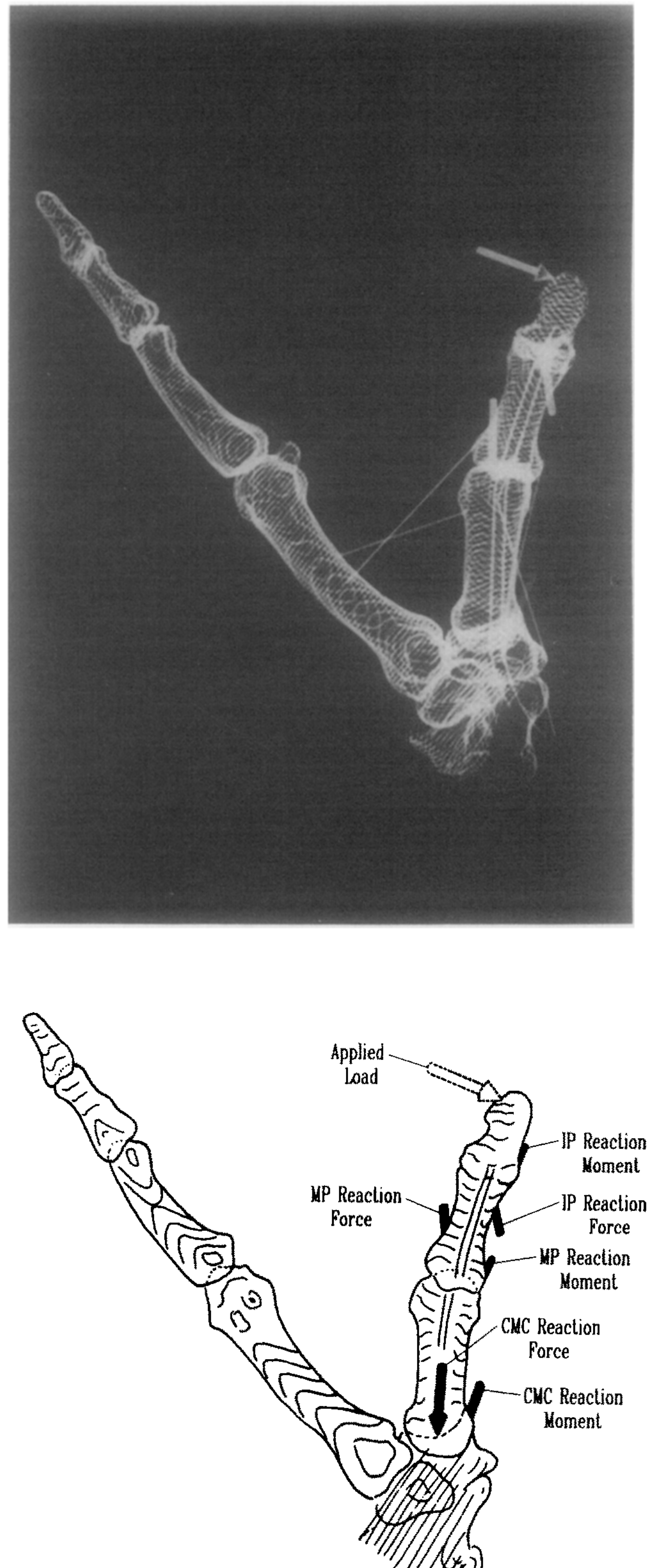

Figure 6 Computer visualization of the directions of the joint reactions for the 'wide grasp' posture, solved for an applied load of 10N. Symbols as *Figure 3*

the point where the metacarpal pivots on the flexor carpi radialis' insertion onto the second metacarpal.

Cooney *et al.*[12] recorded electromyographs for thumb muscles during various pinches and grasp. They determined that during tip pinch the ADP, the FDI, the OPP, and the FPL were active. For grasp the OPP, the ADP, the EPL, and the FDI were active, and for key pinch, the ADP, the FPL, the OPP, the EPL and the FDI become active. The virtual five-link model predicted the adductors (FDI and ADP), the FPL, and the APL act in concert to stabilize the thumb for tip pinch. For wide grasp, the EPB, ADP, OPP and the FDI stabilized the thumb. In key pinch, the flexors, the EPB, the APL and the APB are activated. The virtual five-link model of the thumb predicted similar recruitment patterns to Cooney's EMG data except for

Table 1 Muscle forces (N) predicted by the virtual five-link model for an applied load of 10 N

Muscle	Key pinch	Screwdriver	Tip pinch	Wide grasp
FPL	67.8	93.7	24.4	0.0
FPB	48.5	34.7	0.0	0.0
EPL	0.1	28.8	0.0	1.7
EPB	71.7	71.3	5.1	15.9
OPP	0.0	0.0	1.4	78.3
ADP	0.0	0.0	14.5	34.3
APL	7.5	0.0	25.4	0.0
APB	5.7	16.9	0.0	0.0
FDI	0.0	0.0	13.6	8.6

Table 2 Joint force (N) predicted by the virtual five-link model for an applied load of 10 N

Distal surface of	Key pinch	Screwdriver	Tip pinch	Wide grasp
Trapezium (CMC reaction force)	188.5	241.1	61.5	129.2
Metacarpal (MP reaction force)	181.7	239.1	33.8	49.1
Proximal phalanx (IP reaction force)	65.4	128.5	18.8	11.4

Table 3 Joint moments (N.mm) predicted by the virtual five-link model for an applied load of 10 N

Distal surface of	Key pinch	Screwdriver	Tip pinch	Wide grasp
Trapezium (CMC reaction moment)	468.8	578.6	487.1	1597.0
Metacarpal (MP reaction moment)	977.3	1241.2	280.5	377.2
Proximal phalanx (IP reaction moment)	229.2	293.1	164.2	201.6

the key pinch posture. In our study, the thumb was not as abducted as in the Cooney[12] study, therefore the OPP and ADP were activated to stabilize the thumb.

The force applied to the surface of the trapezium as a result of the thumb muscles firing to stabilize an applied load was between 6 and 24 times the applied load depending on the posture of the thumb. Previous results published by Cooney and Chao[2] predicted forces applied to the trapezium of 12 times the applied load. For key pinch and screwdriver hold the virtual five-link model of the thumb predicted loads of 79% greater magnitude than predicted by Cooney and Chao. The average load applied to the trapezium was 29% greater.

Although only four physiologic positions were analysed in the paper, any position can be studied. The model also has the ability to add or subtract functioning muscles. With this capability, paralysis due to trauma or disease can be modelled. Likewise, tendon transfers can be simulated to attempt to re-balance the system created by the paralysis. Finally, the model can be used as a base of information for the design and development of CMC prostheses.

REFERENCES

1. Chao EY, Opgrande JD, Axmear FE. Three dimensional force analysis of finger joints in selected isometric hand function. *J Biomech* 1976; **19(6)**: 387–396.
2. Cooney WP, Chao EY. Biomechanical analysis of static forces in the thumb during hand function. *J Bone Joint Surg* 1977; **59-A(1)**: 27–36.
3. Hollister A, Buford WL, Myers LM, Giurintano DJ, Novick A. The axes of rotation of the thumb carpometacarpal joint. *J Orthop Res* 1992; **10(3)**: 454–60.
4. Buford WL, Myers LM, Hollister AM. A modeling and simulation system for the human hand. *J Clin Eng* 1991; **15(6)**: 445–51.
5. Thompson DE, Giurintano DJ. A kinematic model of the flexor tendons of the hand. *J Biomech* 1989; **22(4)**: 327–34.
6. Landsmeer JMF. Studies in the anatomy of articulation. *Acta Morphol Neerl Scand* 1961; **3**: 287–321.
7. McPhate AJ. Mechanical design using nonderivative search and quadratic penalty functions, *Oklahoma State Applied Mechanics Conference*, 1975; paper 18.
8. Powell MJD. An efficient method for finding the minimum of a function of several variables without calculating derivatives. *Computing J* 1964; **7**: 155–62.
9. Brand PW, Beach RB, Thompson DE. Relative tension and potential excursion of muscles in the forearm and hand. *J Hand Surg* 1981; **6-A(3)**: 209–19.
10. Crowninshield RD, Brand RA. A physiologically based criterion of muscle force prediction in locomotion. *J Biomech* 1981; **14(11)**: 793–801.
11. Myers LM, Buford WL, Giurintano DJ, Thompson DE. Interactive segmentation of three-dimensional anatomical data for musculoskeletal modeling, *Proceeding of 9th Annual National Computer Graphics Association* 1988; **III**: 143–51.
12. Cooney WP, An KN, Daube JR, Askew LJ. Electromyographic analysis of the thumb: a study of isometric forces in pinch and grasp. *J Hand Surgery* 1985; **10-A(2)**: 202–10.